

The OVLA 1.5-m primary as a segment for an Extremely Large Telescope ?

L. Arnold, O. Lardière

CNRS - Observatoire de Haute-Provence, 04 870 Saint-Michel-l'Observatoire, France
E-Mail: arnold@obs-hp.fr

J. Dejonghe

Laboratoire d'Astrophysique Observationnelle, Collège de France,
04 870 Saint-Michel-l'Observatoire, France

The Optical Very Large Array (OVLA) 1.5 *m* prototype telescope is under construction at Observatoire de Haute Provence. This telescope features a thin active parabolic $f/1.7$ mirror, weighting 100 kg/m^2 with the active cell. The meniscus-shaped mirror, made of low-cost ordinary window glass, is 24.1 mm thick and supported by 32 actuators, each ensuring both axial and lateral supporting *via* a glued triple contact point under the mirror. The active optics system is briefly described. We discuss the characteristics of this mirror concept (weight, low-cost, thermal behaviour, wind buffeting) versus its application to Extremely Large Telescope primary mirror active segments.

Key words: active optics, segmented mirror, ELT

1. Introduction

The Optical Very Large Array (OVLA)¹ of $N = 27$ or more 1.5 *m* telescopes is expected to achieve efficient high-resolution imaging in the $400 - 3300 \text{ nm}$ range. In the *densified pupil* mode², it will provide snap-shot images containing N^2 resolved elements, 10^{-4} arc-second wide in yellow light. An OVLA prototype telescope is under construction at Observatoire de Haute Provence (OHP). After tests at OHP, this telescope will be connected to the GI2T interferometer³, to upgrade this instrument to 3 telescopes.

After a brief presentation of the OVLA telescope active mirror system, we put emphasis on several points interesting its use as an Extremely Large Telescope (ELT) primary mirror segment: weight, low-cost, wind buffeting and thermal behaviour.

2. The OVLA unit telescope active M1

A. Overview

Each telescope is an afocal Gregory telescope with a beam compression of 20 and a 1.5 *m* primary mirror (figure 1). For compactness, the focal ratio of the primary is $f/1.7$ and the complete telescope is housed in a 2.8 *m* sphere, according to the "téléscope boule" concept developed by Labeyrie for GI2T³.

The on-board optics must be as light as possible because the telescope is expected to be movable in the next future to maintain a zero OPD during the observation. The meniscus-shaped $f/1.7$ M1 is thus only 24.1 mm thick, with a mass of $\sim 100 \text{ kg}$. Table 1 gives M1 main features.

B. Active axial supports

M1 is supported by 29 actuators and 3 fixed points. Each carries a triangle providing $3 \times 32 = 96$ points of support. Each contact point is glued on the mirror back side.

The axial force to be applied to the mirror by each actuator is typically 30 N and must be controlled to within $\sim 0.1 \text{ N}$ to avoid wavefront deformations larger than 50 nm RMS . The actuator sensitivity is $\sim 0.04 \text{ N}$, but the absolute value of the force is known only within $+/- 1 \text{ N}$, apparently due to loadcell offset slow (one day) variations. Since the corrections are done in a differential way (i.e. we apply force *variations*), the exact force value is much less

useful than having a good sensitivity. The force is produced by a spring compressed by a screw that is moved up and down by a small DC motor.

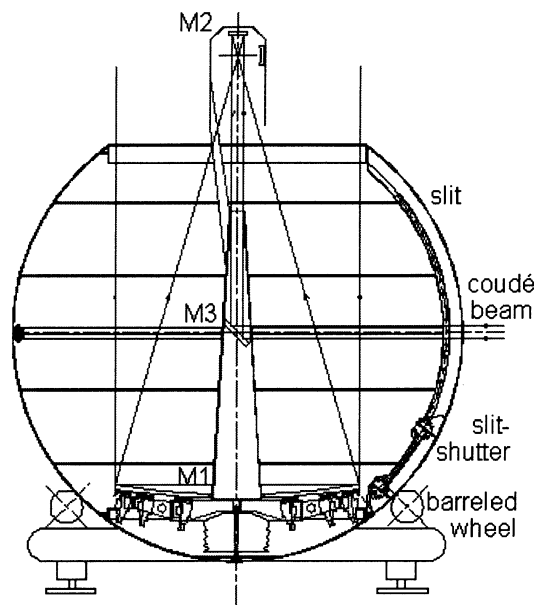


Fig. 1. View of the prototype telescope in its 2.8 m spherical mount. The $f/1.7$ meniscus-shaped parabolic M1, concave gregorian parabolic M2 and flat M3 mirrors are visible. M1 and M2 are both active: M2 controls focus and coma *via* three position actuators, while M1 is used to control other low order modes with 29 force actuators.

Table 1. OVLA M1 main features

Parameter	Value
Outer diameter	1.52m
Inner diameter	0.35m
Thickness	24.1mm
Mirror substrate	standard window glass
Coef. of thermal expansion (CTE)	$9 \times 10^{-6} \text{ } ^\circ\text{C}^{-1}$
Shape	meniscus
f/ ratio	1.7

C. Passive lateral supports

Supporting the mirror only by the edge as it is done for recent 8 m telescopes is very difficult: in a spherical mount with the Coudé beam tracking (or in an equatorial mount), gravity does not relate to the mirror as does in an alt-az mount. Sophisticated lateral supports of 8 m telescope would then become even more complicated. Moreover, there is little room around the mirror when it is installed in the sphere, and there will be none in an ELT. The lateral supporting forces are thus applied across the 96 glued contact points. The largest force amounts to $\sim 10 N$ per point (mirror pointing the horizon) and the required accuracy is $0.6 N$ peak to valley. These forces are applied passively using a lever and a counterweight.

A detailed description of the axial and lateral support is given in Ref. 1.

D. Modal correction

The force variations are derived from wavefront sensing and pre-calibrated tables of 29 forces for each mirror mode. The modes have been computed using an analytical model of the meniscus-shaped mirror⁴ and figure 2 shows the first four mirror modes (among 29) computed after a Singular Value Decomposition of the Actuator Influence Functions matrix⁵.

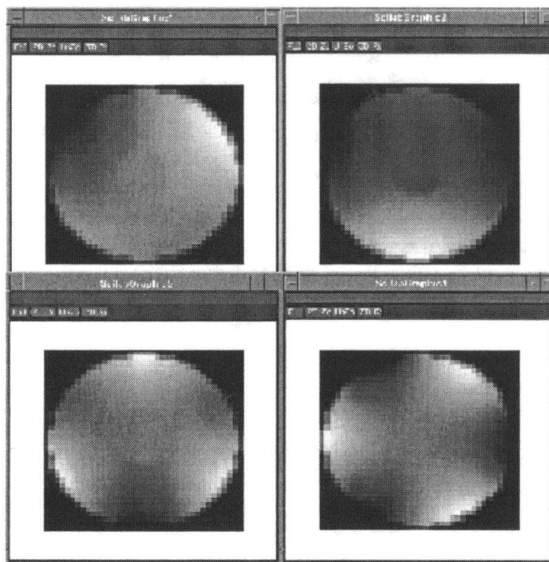


Fig. 2. Grayscale view of the first four computed mirror modes excited by the 29 actuators. Mode 1 (upper left) features mixed Zernike Z_5 (astigmatism) and tilt, while the mode 2 (upper right) presents a large amount of Z_6 (astigmatism). Modes 3 and 4 (lower left and right), are clearly dominated by Z_9 and Z_{10} , respectively.

3. Discussion

A. ELT M1 segment radius of curvature

In the following, we will consider the possibility to use the OVLA M1 segment in two different kinds of 50m ELT: a 4-reflexion ELT, as the swedish⁶ 40m, and a MMT-type ELT, as the one described in Ref. 7 in these proceedings. One of the main differences between these two concepts is the radius of curvature of the M1 segments: In the swedish design, a $f/1.2$ 40m primary would give a radius of curvature for each segment of 96m. In the case of a MMT-type

telescope, the M1 would be an array of parallel telescopes, possibly an array of OVLA telescopes, or an array of 8m VLT-type telescopes, installed on a single mount. In the latter case, the radius of curvature of each segment would be much smaller (5.1m in the case of OVLA telescopes), leading to interesting low and compact designs.

B. Wind buffeting

The first vibrational mode frequency for a thin circular plate is given by⁸

$$f_1 \sim 0.17 \frac{2h}{\pi D^2} \left[\frac{E}{12(1-\nu^2)\rho} \right]^{1/2} \quad (\text{Hz}) \quad (1)$$

where h is the thickness, D the diameter, E the Young modulus, ν the Poisson coefficient and ρ the blank material density. The value for f_1 is 16 Hz for the VLT M1, while reaching 55Hz for the OVLA M1. Measurements done by Noethe *et al.*⁹ showed that the power spectrum of the wind pressure over a dummy 3.5m mirror has a cut-off frequency around 2Hz. This low value suggests that a small segment as the OVLA M1 should not enter in resonance with the wind. For much thinner *adaptive* segments up to 6m in diameter, such as those considered recently by the swedish team¹⁰, f_1 could drop down to 1Hz or less. Hard actuators should therefore be considered (piezo or magneto-strictive for example) rather than soft ones (spring or voicecoil).

OVLA M1 support features soft actuators and therefore is quite sensitive to wind pressure, especially because the fixed points are at mirror edge. Putting these fixed points at normalized radius 0.64 decreases both RMS and peak-to-valley deformations by a factor of ~ 4 . In this configuration, calculations show that a 2.3N/m^2 RMS uniform wind pressure would induce a 125nm RMS trifoil deformation, which may correspond to a wind speed of the order of 3m/s by extrapolating Zago's paper¹¹.

C. Thermal behaviour

The OVLA primary is made of ordinary 25mm window glass from Pilkington, UK, slumped in a special oven to obtain the desired meniscus-shaped blank¹². This blank cost 40 times less than the equivalent meniscus-shaped Zerodur blank. The counterpart of this low price is the very poor thermal behaviour of the window glass: its coefficient of thermal expansion is 3 times larger than for Pyrex-like glasses (table 1), and at least 2 orders of magnitude larger than for Zerodur or ULE materials.

Table 2. Mirror deformations in terms of Z_4 (defocus) and Z_{11} (spherical) of possible M1 segments under thermal loads. Values are for the mechanical surface, not for the wavefront. A constant thermal gradient of $(1/h)^\circ\text{C}/\text{m}$ between the (colder) optical and rear mirror surfaces is assumed. h stands for the mirror thickness. When the radius of curvature is $R = 96\text{m}$, the blanks feature no central hole. Measurements with the OVLA M1 mirror looking at the dark sky showed that the optical surface is never colder than 1°C with respect to the rear surface.

Blanks	Z_4 (m RMS)	Z_{11} (m RMS)
OVLA M1, R=5.18m, h=24mm, window glass	6.56e-6	3.15e-6
OVLA M1, R=5.18m, h=35mm, Pyrex	2.76e-6	0.67e-6
R=96m, Diam.=1.5m, h=24mm, window glass	31.0e-6	12.3e-9
R=96m, Diam.=1.5m, h=35mm, Pyrex	7.43e-6	3.97e-9
R=96m, Diam.=2.3m, h=24mm, window glass	69.9e-6	177.e-9
R=96m, Diam.=2.3m, h=35mm, Pyrex	17.4e-6	27.8e-9

Although the aluminized mirror has a low thermal emissivity, measurements with the OVLA M1 mirror looking at the dark sky showed that the optical surface is always between 0.45 and 0.85°C colder than the rear surface. This thermal gradient coupled with the high CTE (see table 1) leads to a large deformation of the mirror with a significant difference whether the mirror is meniscus-shaped or not, i.e. the radius of curvature is 5m or 96m : the larger the radius of curvature, the smaller the spherical aberration and the larger the defocus. Table 2 and figure 3 give quantitative data for different blank shapes and materials. We have verified in the lab that a $+0.25^\circ\text{C}$ heated rear surface gave a wavefront error of Zernike $Z_{11} = 1800\text{nm RMS}$, in correct agreement with FEA theory giving 1600nm RMS (table 2).

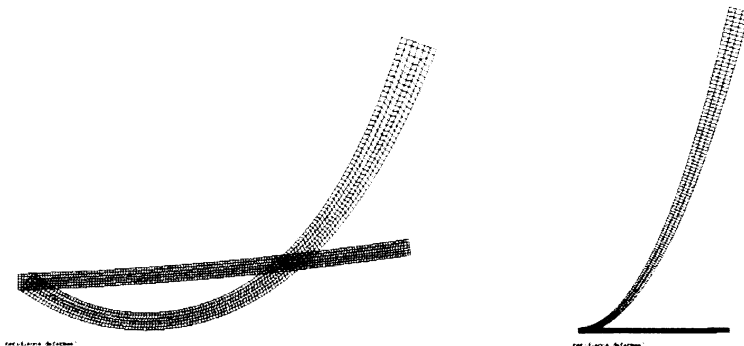


Fig. 3. Half side-view of two mirror blanks under thermal load computed by FEA with Castem2000. A thermal gradient of $(1/h)^\circ\text{C}/\text{m}$ inside the meniscus-shaped blank is considered. The thickness h is 24mm . Left: The OVLA M1, with its $R = 5.18\text{m}$ radius of curvature and its 175mm radius central hole, is represented before and after deformation. The Z_{11} term of the loaded mirror is $3.15\mu\text{m RMS}$ (on mechanical surface, not wavefront). Right: M1 radius of curvature is now $R = 96\text{m}$, there is no central hole, and the Z_{11} term falls to 12nm , while the Z_4 term increases from $6.56\mu\text{m RMS}$ to $31.0\mu\text{m RMS}$. Forces ranging from -240N to $+170\text{N}$ are required to compensate the latter Z_4 term.

Z_{11} is too large to be corrected by the OVLA actuators, but three alternative methods of correction can be considered, either for OVLA or for an ELT made of an array of OVLA telescopes⁷.

The first would be to compensate this quasi-static Z_{11} with an adaptive mirror, possibly the secondary mirror¹³ on OVLA, providing it does not saturate the mirror.

The second solution would be to have an active secondary mirror working as a Z_{11} corrector (in addition to focus and coma). Such correctors can feature only one central actuator, assuming a correct thickness radial profile is given to the mirror, as proposed by Lemaître¹⁴.

A third solution would be a thermal control of the primary. If the thermal gradient is constant, we have to achieve a uniform heating over the entire surface. This can be done by Joule heat dissipation in the Al reflective coating. This is equivalent to requiring that electric field E_y is a constant while $E_x = 0$. The solution is to put a large number of contacts around the edge of the mirror with a voltage that varied as $\sin(\theta)$, where $\theta = 0$ corresponds to the x-axis (figure 4). The same setup of contacts has been chosen by the Gemini team¹⁵ in order to heat the Zerodur 8m surface to avoid local air convection due to the colder optical surface. In the case of the OVLA mirror, we will not only benefit from a reduction of air convection, but also correct the spherical aberration.

Experiments showed that the thermal gradient is in fact not constant, and somewhat 0.1°C smaller near mirror edges. Therefore, a residual Z_{11} will probably subsist, although it becomes within the reach of active or adaptive optics. Note that by putting a voltage between 2 selected contacts would allow to heat only a part of the mirror surface, and therefore generate (or correct) a given deformation (or aberration). This both temporal and spatial low-frequency *thermal active optics* is under study at OHP.

Another solution would be to change the blank material for *Pyrex*, or even *Zerodur* or *ULE*, with the drawback of a much higher cost. But in the case of *Pyrex*, table 2 shows that a 35mm thick *Pyrex* blank would present almost 5 times less spherical aberration than the current OVLA mirror. The residual Z_{11} on the *Pyrex* mirror would be within the reach of adaptive optics, in any case available on an ELT.

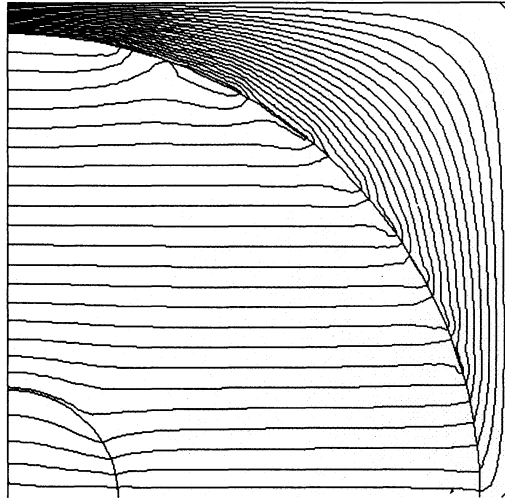


Fig. 4. View of the electric potential lines over the mirror surface obtained with a set of 32 electrodes (28 around mirror edge, 4 around central hole). The voltage applied by each electrode varied as $\sin(\theta)$, where $\theta = 0$ corresponds to the x-axis. Since the lines are almost parallel, E_y is a constant. Thus a constant electric current density providing a constant heat dissipation will be achieved over the entire mirror. This graph has been computed with the TCE Finite Element Software Package¹⁶.

In the case of a longer radius of curvature (here 96m), table 2 shows that Z_{11} becomes very small, but the focus term Z_4 increases and induces a dramatic focus change ϵ given by

$$\epsilon \sim 32\sqrt{3} \left(\frac{f}{D}\right)^2 Z_4 \quad (2)$$

where f/D is the focal ratio of the segment and Z_4 the Zernike focus term *on the glass* (half of the wavefront). The third line of table 2 gives $\epsilon = 1.8m$ for $Z_4 = 31.0\mu m$ corresponding to a difference of $1^\circ C$ between the mirror surfaces. It seems that this focus shift cannot be compensated by simply translating a 'secondary' mirror somewhere as it is usually done. An active control of the segments, either thermal or with force actuators, or both, is required. In the latter case, calculations give forces ranging from $-240N$ to $+170N$ to compensate the Z_4 term of $31.0\mu m$. These forces look reasonable, although they are not applicable by current OVLA actuators (max. range 60N).

D. ELT M1 mass

Current OVLA technology gives a mass of only $\sim 100kg/m^2$ for the mirror and its active support, thanks to the 24mm thick mirror. The mass for a 50m M1 array would be $2 \times 10^5 kg$. Pyrex is 10% lighter, but with 35mm thick segments, the array would have a mass of $2.7 \times 10^5 kg$. Obviously, a more detailed study of the complete mechanics is necessary to deduce a consistent mass estimation, but the masses above are one order of magnitude larger than the mass of the 8m telescopes, although the collecting surface has been increased by two order of magnitude.

E. ELT M1 blanks cost

The cost is definitely the greater advantage of an ELT M1 made of ordinary glass. The flat blanks for a 50m array would cost 0.35 M Euro, according to Pilkington french dealer. Corning France gave us the prices for 55mm thick Pyrex and 35mm thick ULE, respectively 3.9 M Euro and 28 M Euro. Almost exactly one order of magnitude is lost when better mirror substrates are chosen, but this cost increase should nevertheless be compared with the total cost of the ELT.

An interesting point to note is the significant decrease of cost if thinner segments are chosen (obviously because less material is necessary). For an adaptive M1 array, made of 300mm segments for example, the cost of the blanks would decrease by a factor of 15 for thickness $\leq 10\text{mm}$ and a factor of 40 for thickness $\leq 5\text{mm}$ for *Pyrex* and *ULE*. The decrease is less significant for ordinary glass, i.e. the cost decreases by a factor of 3 for thickness $\leq 10\text{mm}$ and a factor of 4 for thickness $\leq 5\text{mm}$.

4. Conclusion

We have shown that the use of ordinary window glass for ELT M1 segments leads to serious difficulties, above all due to the very poor thermal behaviour of this low-cost material. Nevertheless, in the case of a MMT-type array with segments having a small f/λ ratio, the spherical aberration of thermal origin could be controlled *via* an adaptive secondary, an active Z_{11} -corrector secondary, or with a heating of the Al coating. In the case of a much larger radius of curvature, a large defocus of thermal origin occurs on each segment and it has to be controlled with actuators, possibly coupled again with an heating of the Al coating. *Pyrex*-like or *Zerodur*-like materials could obviously simplify or solve, respectively, this problem. Further studies on the possibility to use standard window glass, for 300mm diameter adaptive segments for example, should be motivated by the fact that this material is two orders of magnitude cheaper than *Zerodur* or *ULE*.

Acknowledgments: This research was supported by the *Région Provence-Alpes-Côte d'Azur*, the *Institut National des Sciences de l'Univers (INSU-CNRS)* and the *Collège de France*.

-
1. J. Dejonghe, L. Arnold, O. Lardière, J.P. Berger, C. Cazalé, S. Dutertre, D. Kohler, D. Vernet, "The Optical Very Large Array (OVLA) prototype telescope: status report and perspective for large mosaic mirrors", SPIE Proc. vol. 3352, 603-613, 1998.
 2. A. Labeyrie, "Resolved imaging of extra-solar planets with future 10-100 km optical interferometric arrays", *Astron. & Astrophys. Suppl. Ser.*, vol. 118, 517-524, 1996.
 3. D. Mourard, I. Tallon-Bosc, A. Blazit, D. Bonneau, G. Merlin, F. Morand, F. Vakili, A. Labeyrie, "The GI2T interferometer on Plateau de Calern", *Astron. & Astrophys.*, vol. 283, 705-713, 1994.
 4. L. Arnold, "Influence functions of a thin shallow meniscus-shaped mirror", *Applied Optics*, vol. 36, 2019-2028, 1997.
 5. H.M. Martin, W.B. Davison, S.T. DeRigne, J.M. Hill, B.B. Hille, R.L. Meeks, T.J. Trebisky, "Active support optimization for a 3.5-m honeycomb sandwich mirror", SPIE Proc. vol. 2199, 251-262, 1994.
 6. Ardeberg A., Andersen A., Owner-Petersen M., "Choice of aperture for large telescopes for optical wavelengths", in SPIE Proc. vol. 3352, 754-765, 1998.
 7. L. Arnold, "A Multiple-Mirror-Telescope concept for a very compact 50-m Extremely Large Telescope", these proceedings.
 8. R.N. Wilson, F. Franza, L. Noethe, B. Buzzoni, "Active Correction of Wind-Buffering of Thin Telescope Primaries in the Extended Active Optics Bandpass", *PASP*, vol. 105, 1175-1183, 1993.
 9. L. Noethe, X. Cui, S. Stanghellini, "ESO VLT Primary Mirror Support System", in *ESO Proc. 'Progress in Telescope and Instrumentation Technology'*, M.H. Ulrich, Ed., 195-198, 1992.
 10. T. Andersen, private communication, 1999.
 11. L. Zago, "The design of telescope enclosures for the VLT", in *ESO Proc. 'Progress in Telescope and Instrumentation Technology'*, M.H. Ulrich, Ed., 235-246, 1992.
 12. L. Arnold, B. Dejonghe, J. Dejonghe, A. Labeyrie, "Producing mirrors for the Optical Very Large Array", *ESO Conf. on 'Progress in Telescope and Instrumentation Technologies'*, M.H. Ulrich, Ed., 269-272, 1992.
 13. D.D. Walker, J.H. Lee, R.G. Bingham, D. Brooks, M. Dryburgh, G. Nixon, H. Jamshidi, S.W. Kim, B. Bigelow, "Rugged adaptive telescope secondaries: experience with a demonstrator mirror", in SPIE Proc. vol. 3353, 872-878, 1998.
 14. G. Lemaître, "Sur la flexion des miroirs secondaires de télescopes", *Nouv. Rev. Optique*, vol. 7, 389-397, 1976.
 15. B. Perona, E. Hansen, D. Hagelbarger, A. Rudeen, "Hardware implementation of the mirror surface heating system for the Gemini 8 meter telescopes", in SPIE Proc. vol. 3352, 868-878, 1998.
 16. *Field Precision*, Finite-Element software for Electromagnetics. Contact: Prof. Stanley Humphries, Dpt of Electrical and Computer Engineering, U. of New Mexico, Albuquerque, NM 87131, humphrie@warlock.eece.unm.edu, www.fieldp.com.